Extended Abstract

One-dimensional Simulation of Dielectric Barrier Discharge at Atmospheric Pressure in Nitrogen Gas with the Addition of 10% Oxygen

Azadeh Barjasteh*

Department of Physics, Faculty of Basic Science, Lorestan University, Khoram Abad, Iran

Received: 28.06.2025 Final revised: 30.06.2026 Accepted: 01.09.2026 Published On-Line: 05.09.2026

Doi: 10.22055/jrmbs.2026.20969

Abstract

Dielectric barrier discharges with a nitrogen-oxygen gas mixture are of great interest due to their positive effects on surface modification and sterilization. Among all the mixtures, the 90% nitrogen-10% oxygen gas mixture is of great importance due to its plasma stability and strong chemical activity. In this study, a one-dimensional fluid model is used to investigate the physicochemical characteristics of dielectric barrier discharge in a 90% Nitrogen-10% Oxygen gas mixture at atmospheric pressure. For this purpose, the COMSOL code is used to investigate the discharge characteristics, including the current-voltage curve and the generation and destruction of active particles under a sinusoidal voltage with an amplitude of 8 kV and a frequency of 10 kHz. The simulation showed that this combination does not turn into an arc, spark, or filament discharge, while producing a relatively stable plasma. Also, the simulation results showed that the most abundant ion in the discharge space is the O_2^+ ion, while only ten percent of the total gas is oxygen. Also, the most abundant active particles at this moment were oxygen atoms, NO molecules, and ozone molecules, respectively, which makes this gaseous mixture a suitable mixture for sterilization and surface modification processes.

Keywords: Dielectric Barrier Discharge, Nitrogen discharge simulation, discharge properties

* Corresponding Author: Barjasteh.a@lu.ac.ir

This work is licensed under a Creative Commons Attribution 4.0 International License

1. INTRODUCTION

Dielectric barrier discharges are currently gaining popularity for applications such as medical [1], agriculture [2], and food packaging [3], etc. Dielectric barrier discharges are created when at least one dielectric layer is placed in the discharge space between two electrodes, one of which is connected to an oscillating voltage. This dielectric layer prevents arcing or sparking and creates a cold plasma. The oscillating voltage also causes the electrons to gain enough energy to ionize gas atoms and molecules, and after the charged particles accumulate on the dielectrics, when a field is established in the opposite direction to the initial field, the voltage direction is reversed, and the discharge continues. At atmospheric pressure, especially when electrical discharges are generated without a vacuum pump and no pre-pumping process is performed before the injection of the main gases, there is a small amount of oxygen in the discharge space, which can affect the discharge characteristics [4]. For the successful application of electrical discharges, and a better understanding of the interactions between plasma and materials, plasma parameters must be obtained experimentally or by simulation. This is important when plasma is used for surface modification or sterilization because, in the case of surface modification, oxygen atoms, metastable nitrogen particles, and NO molecules play a fundamental role and cause various reactions with the surface, including breaking surface bonds or exciting the surface and forming functional groups [4]. Meanwhile, active oxygen and nitrogen particles play a major role in sterilization processes. Studies show that adding oxygen gas to an electric discharge in noble gases can increase the antimicrobial effect of electric discharges due to the increased presence of active oxygen and nitrogen particles [5, 6]. Therefore, it is of particular importance to investigate the changes in various particles in plasma, including metastable particles and active oxygen and nitrogen particles, for the optimization of surface processes by plasma and antimicrobial effects. Among the different nitrogen and oxygen gas compositions, the 90% nitrogen-10% oxygen composition was chosen for this study because, in this case, the amount of oxygen is so low that the plasma remains stable and so high that the plasma is highly active. In this article, using COMSOL software, the effect of oxygen presence on dielectric barrier discharge characteristics, including the density of electrons, ions, metastable particles, and plasma radiation, is investigated, and it is concluded that a gas mixture of 90% nitrogen-10% oxygen can be a suitable mixture for sterilization processes.

2. SIMULATION

In this study, a one-dimensional simulation of an electric discharge with a dielectric barrier in a 90% nitrogen-10% oxygen gas mixture at atmospheric pressure was performed to generate a plasma with a sinusoidal voltage of 8 kV amplitude and 10 kHz frequency. In this simulation, the average electron density and energy were calculated by solving the pair of propulsion and diffusion equations according to the following relations:

$$\frac{\partial n_e}{\partial t} + \nabla.\vec{\Gamma}_e = R_e - (\vec{u}.\nabla)n_e \quad (1)$$

$$\vec{\Gamma}_e = -(\vec{\mu}.\vec{E})n_e - D_e.\nabla n_e \quad (2)$$

In these equations, n_e is the electron density; $\vec{\Gamma}_e$ is the electron flux; $\vec{u}$ is the average velocity of the species; R_e is the electron production rate; and D_e is the electron diffusion coefficient. Equation 3 shows the energy rate due to inelastic collisions, and equation 4 shows the electron energy density.

$$R_\varepsilon = S_{en} + (Q + Q_{gen})/q \quad (3)$$

$$\frac{\partial n_\varepsilon}{\partial t} + \nabla.\vec{\Gamma}_\varepsilon + \vec{E}.\vec{\Gamma}_e = R_\varepsilon - (\vec{u}.\nabla)n_\varepsilon \quad (4)$$

In these relations, the energy rate of inelastic collisions is R_ε, Q is the main source of heat, and Q_{gen} is the electron energy density. For ionic species, the continuity equation is solved in the form of Equation 5:

$$\frac{\partial n_i}{\partial t} + \nabla.(n_i\vec{u}) = -\nabla.(\mu_i n_i q_i \nabla\varphi - D_i \nabla n_i) + S_i \quad (5)$$

In this equation, S_i is the ion production source, n_i is the ion density, and φ is the electrostatic potential. The emission of secondary electrons from collisions between ions and metastable particles is considered as the boundary condition. Equations 6 and 7 are the accumulation boundary conditions, respectively. They show the surface charge of the walls and the conservation of charge in the dielectric region.

$$\frac{\partial \sigma_s}{\partial t} = n J_i + n J_e \quad (6)$$

$$D = \varepsilon_0 \varepsilon_r E \quad (7)$$

In equation 6, parameters σ_s, n, J_i, and J_e represent the surface charge, the unit vector normal to the surface, the ionic charge flux, and the electron charge flux impinging on the surface, respectively.

Also, in equation 7, parameters D, ε_0 ; ε_r , and E represent the electric displacement, the vacuum permittivity, the relative permittivity, and the electric field, respectively.

The geometry of this discharge, shown in Figure 1, consists of two circular electrodes with an area of 0.01 m^2, each of which is covered with a dielectric of AL_2O_3 with a thickness of 0.5 mm and a dielectric constant of 8, which are separated by 1 mm. The set of particles considered for this simulation includes electrons**,** N_2^+, N_3^+, N_4^+, O_2^+, O_2^-, O^+, NO^+, N_2A, N_2a, N_2B, N_2C, ND, N, O_3, O and NO, among which N_2A and N_2a particles are metastable particles and N_2B and N_2C are nitrogen radiative particles. Also, the initial values are $10^{13}/m^3$ for the electron density, $5\times10^{13}/m^3$ for the N_4^+ ion density, $2\times10^{11}/m^3$ for the N_3^+ ion density, and $1\times10^{11}/m^3$ for the N_3^+ ion density. O_2^+, O_2^-, and O^+ ions, and $1\times10^{10}/m^3$ are considered as NO^+ ions. In this simulation, the gas pressure is 1 atmosphere, and its temperature is 300 degrees Kelvin.

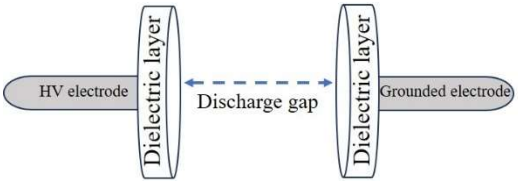


Figure 1. Geometry considered for simulation

Also, 36 reactions were considered for the simulation, and the set of these reactions along with their rates is shown in Table 1. For electron reactions, the reaction cross section was used, which is obtained from www.Lxcat.net. This simulation is based on a set of relationships that are fully stated in reference [7]. Also, for the electron equations, boundary conditions must be considered on the dielectric boundary, which is considered by introducing secondary emission of electrons due to collisions of ions and metastable particles. For this simulation, the secondary emission coefficient for ions and metastable nitrogen particles is 0.01.

Table 1. Set of reactions considered for simulation along with their rates

Reaction Number	**Reaction**	**Reaction Rate(cm^3/s)**
R_1	$e+N_2 \Rightarrow N_2^+ +2e$	*f(E/N)*
R_2	$e+N_2 \Rightarrow e+N_2A$	*f(E/N)*

R3	$e+N_2 \Rightarrow e+N_2a$	*f(E/N)*
R_4	$e+N_2 \Rightarrow e+N_2B$	*f(E/N)*
R_5	$e+N_2 \Rightarrow e+N_2C$	*f(E/N)*
R_6	e+N2+=>2N	$2.8\times10^{-7}(T_g/T_e)^{0.5}$
R_7	$N_2^+ + N_2A \Rightarrow N_3^+ + N_2$	3×10^{-10}
R_8	$N_4^+ + N_2 \Rightarrow N_3^+ + 2N_2$	3.4×10^{-15}
R_9	$N_4^+ + e \Rightarrow N_2C + N_2$	$2\times10^{-6}(T_g/T_e)^{0.5}$
R_{10}	$N_2+N_2a \Rightarrow N_2+N_2$	2×10^{-13}
R_{11}	$N_2+N_2a \Rightarrow N_2B+N_2$	2×10^{-13}
R_{12}	$N_2a+N_2a \Rightarrow N_4^+ + e$	1×10^{-11}
R_{13}	$N_2a+N_2A \Rightarrow N_4^+ + e$	1.5×10^{-11}
R_{14}	$N_2A+N_2A \Rightarrow N_2C+N_2$	3×10^{-10}
R_{15}	$N_2A+N_2A \Rightarrow N_2B+N_2$	7.7×10^{-11}
R_{16}	$N_2C \Rightarrow N_2B+hv$	2.7×10^{7}
R_{17}	$N_2C+N_2 \Rightarrow N_2a+N_2$	1×10^{-11}
R_{18}	$N_2B \Rightarrow N_2A+hv$	1.5×10^{5}
R_{19}	$N_2B+N_2 \Rightarrow N_2A+N_2$	5×10^{-11}
R_{20}	$e+O_2 \Rightarrow O_2^+ + 2e$	*f(E/N)*
R_{21}	$e+O_2 \Rightarrow O_2^-$	*f(E/N)*
R_{22}	$e+O_2^+ \Rightarrow 2O$	4.8×10^{-7}
R_{23}	$O_2^- + O \Rightarrow O_3 + e$	1.5×10^{-10}
R_{24}	$O+O_3 \Rightarrow O_2+O_2$	8.3×10^{-15}
R_{25}	$N_2^+ + O_3 \Rightarrow N_2 + O_2^+ + O$	1×10^{-10}
R_{26}	$N_2^+ + O_2 \Rightarrow N_2 + O_2^+$	$6\times10^{-11}(T_g/T_e)^{0.5}$
R_{27}	$N_4^+ + O_2 \Rightarrow 2N_2 + O_2^+$	2.5×10^{-10}
R_{28}	$N_2^+ + O \Rightarrow NO^+ + N$	$1.3\times10^{-10}(T_g/T_e)^{0.5}$
R_{29}	$N_4^+ + O \Rightarrow O^+ + 2N_2$	2×10^{-10}
R_{30}	$N_2A+O_2 \Rightarrow O+O+N_2$	2.5×10^{-12}
R_{31}	$N_2A+O \Rightarrow N+NO$	7×10^{-12}
R_{32}	$N_2A+NO \Rightarrow NO+N_2$	7×10^{-11}
R_{33}	$N_2a+O_2 \Rightarrow O+O+N_2$	2.8×10^{-11}
R_{34}	$N_2a+NO \Rightarrow N+O+N_2$	3.6×10^{-10}
R_{35}	$N_2B+O_2 \Rightarrow O+O+N_2$	3×10^{-10}

R_{36}	$N_2C+O_2=>O+O+N_2$	3×10^{-10}

3. RESULTS

Figure 2 shows the current-voltage curve for an electric discharge with a dielectric barrier in a mixture of 90% nitrogen and 10% oxygen. As can be seen, for this gas mixture, the discharge is still in a uniform state because the amount of oxygen is not yet high enough to take the discharge out of the uniform state and drive it towards a filament or spark discharge. In fact, the 90% nitrogen-10% oxygen mixture creates an optimum point where the plasma remains stable but is also highly active.

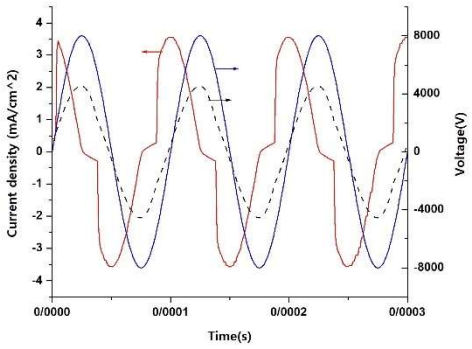


Figure 2. Current-Voltage curve for discharge with a combination of 90% nitrogen-10% oxygen

Figure 3 (a) shows the changes in electron density, and Figure 3 (B) shows the changes in electric field in the discharge space and dielectrics. As can be seen in this figure, in each cycle, electrons produced by ionization processes in the discharge space accumulate on one dielectric. Meanwhile, positive ions are concentrated on the opposite dielectric to create a secondary electric field, greatly reducing the field inside the discharge space. Therefore, the electric field in the discharge space decreases. On the other hand, according to Figure 3 (a), an electron avalanche starts from the middle of the discharge space towards the dielectrics to create an electric discharge. Figure 4 shows the logarithmic plot of the root mean square of various ions in (a) pure nitrogen discharge and (b) discharge with a composition of 90% nitrogen-10% oxygen in terms of discharge space. As can be seen in these figures, in the 90% nitrogen-10% oxygen discharge, O_2^+ particles have the highest number of ions throughout the discharge process, while only 10% of the total gas is oxygen. This result states that despite the very low percentage of oxygen, its amount dominates in the discharge because the ionization energy of oxygen molecules is of the order of 12.07 eV, while the ionization

energy of nitrogen molecules is of the order of 15.58 eV. Therefore, with less energy expenditure, oxygen molecules can be ionized. Thus, their number dominates during the discharge process. In a pure nitrogen discharge, the N_3^+ ions are the least numerous, while in a 90% nitrogen-10% oxygen discharge, the O^+ ions are the least numerous.

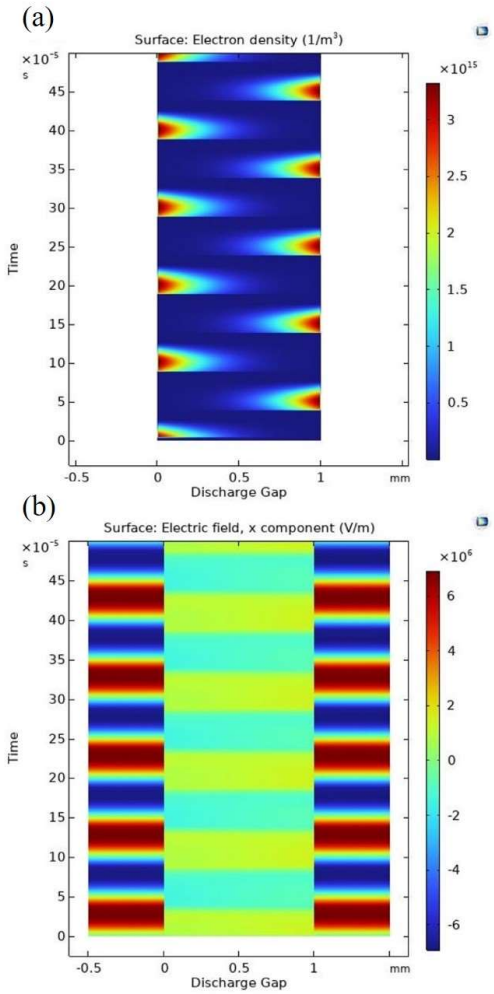


Figure 3. (a) Changes in electron density and (b) Changes in electric field in the discharge space

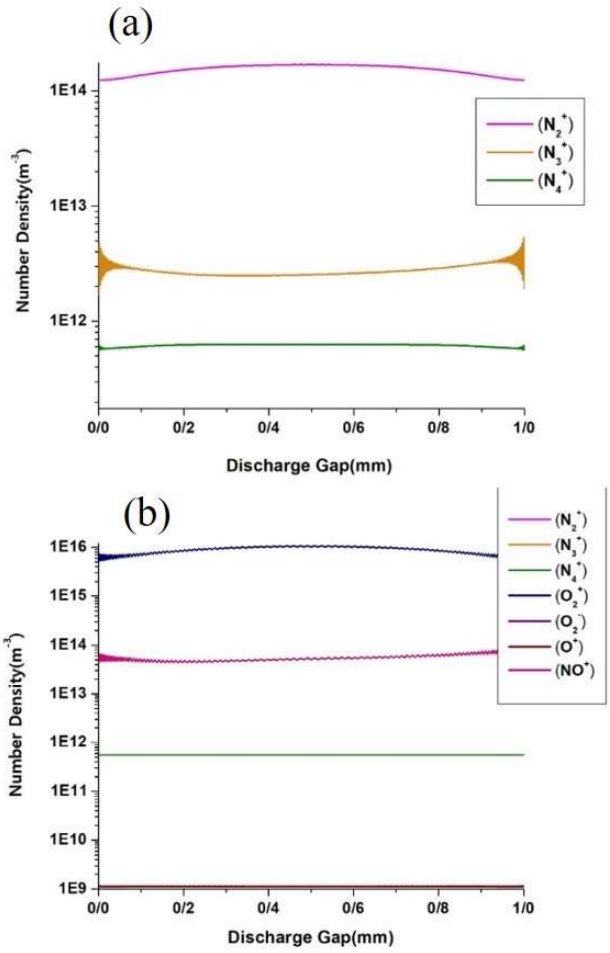


Figure 4. Logarithmic plot of root-mean-square ion density versus distance in (a) pure nitrogen discharge and (b) 90% nitrogen-10% oxygen discharge.

Therefore, in practice, oxygen enters chemical reactions more quickly. Also, in many reactions, including $e+O_2^+ \Rightarrow O+O$, $N_2A+O2 \Rightarrow N_2+O+O$, $N_2a+O_2 \Rightarrow N_2+O+O$, $N_2a+NO \Rightarrow N+O+N_2$, $O_2+N_2B \Rightarrow N_2+O+O$, $N_2C+O_2 \Rightarrow N_2+O+O$, oxygen radicals are produced, which are highly active. These particles produce NO^+ ions through the reaction $N_2^+ + O \Rightarrow NO^+ + N$. Thus, in the discharge of 90% nitrogen-10% oxygen, the density of these ions also dominates. Figure 5 also shows the root-mean-square electron density in discharge with pure nitrogen gas (dashed line) and discharge with a gas mixture of 90% nitrogen-10% oxygen. As can be seen in this figure, the electron density increases slightly with the addition of 10% oxygen. This result has also been confirmed for low oxygen levels

in reference [8]. This phenomenon is because, at low oxygen levels, the number of oxygen atoms is not sufficient to absorb electrons through electronegativity. Also, considering the lower ionization energy of oxygen molecules (12.07 eV) compared to nitrogen molecules (15.58 eV), adding a small amount of oxygen can help produce more electrons through ionization of more oxygen molecules.

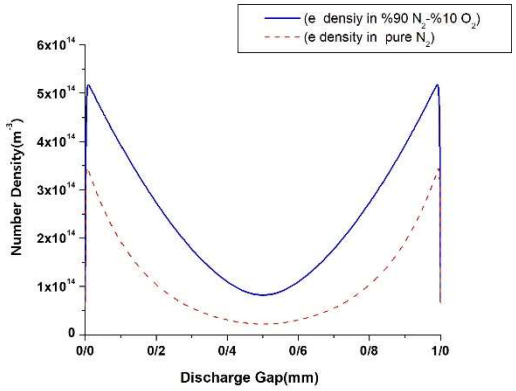


Figure 5. Comparison of the root mean square electron density in pure nitrogen discharge (dashed line) and 90% nitrogen - 10% oxygen discharge (solid line)

Figure 6 shows the spatiotemporal evolution of metastable particles in the discharge space. As can be seen in this figure, the density of both types of nitrogen metastable particles, N_2A and N_2a, on the dielectrics reaches its maximum value. This is while the initial mole fraction for these particles is very low and is considered to be of the order of $1e^{-11}$. These particles play a very important role in the production of electrons and N_4^+ ions through Penning ionization according to the R_{12} and R_{13} reactions. Their maximum presence on the dielectrics leads to the maximum production of electrons in these regions. For comparison, the root-mean-square density of metastable particles for nitrogen discharge and discharge with a gas composition of 90% nitrogen-10% oxygen is plotted in Figure 7. As can be seen in this figure, the presence of 10% oxygen gas significantly increases the density of N_2a metastable particles and decreases the density of N_2A particles in the vacuum space. This result is because the N_2A metastable particles participate extensively in the reaction with oxygen atoms and molecules (R_{30}, R_{31}, and R_{32}) to produce oxygen free radicals. These particles also produce N_2B and N_2C emitting particles through R_{14} and R_{15} reactions. Therefore, the plasma emissions are also expected to be higher in the regions close to the dielectrics per half cycle. The correctness of this

result is shown in Figure 8. To compare the plasma emissions in a pure nitrogen discharge and a discharge with a composition of 90% nitrogen-10% oxygen, the root-mean-square number density of N_2B and N_2C particles is plotted in Figure 9. As can be seen in this figure, the plasma emissions in a pure nitrogen discharge are higher than those in a plasma with a composition of 90% nitrogen-10% oxygen. This phenomenon is because, in the 90% nitrogen-10% oxygen discharge, the excited N_2B and N_2C particles participate extensively in the R_{35} and R_{36} reactions to react with oxygen molecules, breaking them into oxygen atoms. Therefore, adding 10% oxygen to the nitrogen discharge reduces plasma emissions. Among the active oxygen species, ozone causes cell death of microorganisms by oxidizing their cell walls.

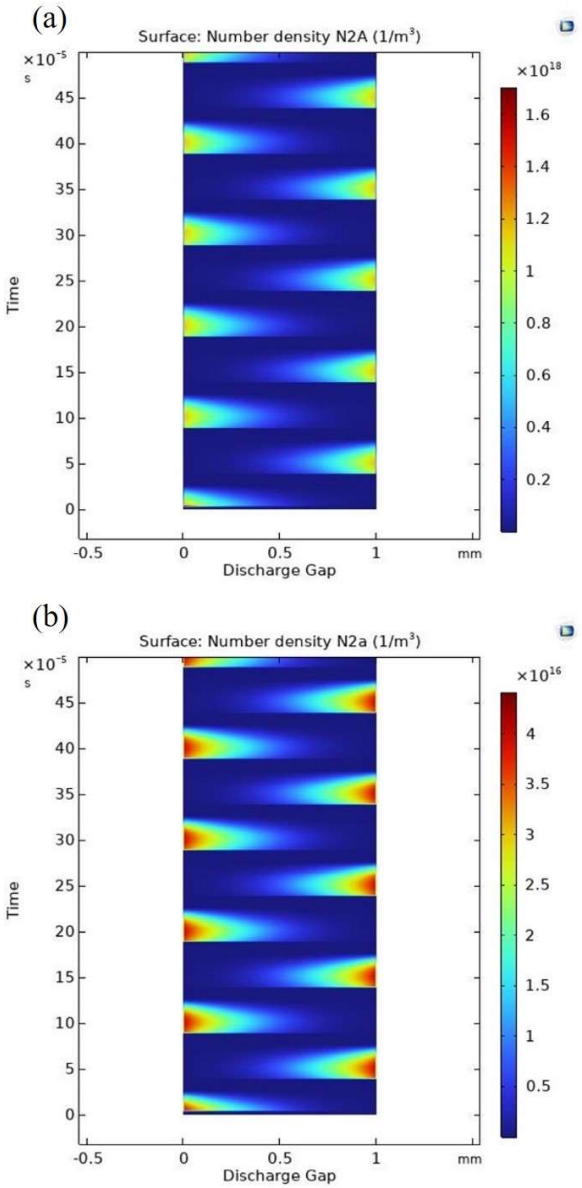


Figure 6. Spatio-temporal evolution of metastable particles (a) N_2A and (b) N_2a

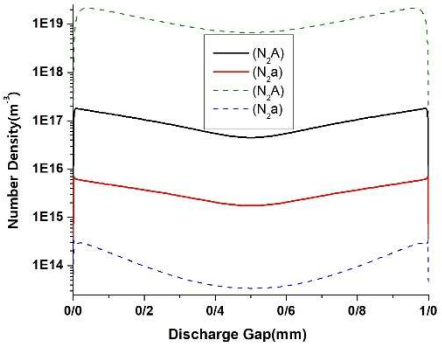


Figure 7. Logarithmic diagram of the distribution of metastable particles at the moment of maximum flow for discharge with pure nitrogen gas (dashed line) and discharge with a gas mixture of 90% nitrogen - 10% oxygen (solid line)

Thus, this particle plays an important role in sterilization and pollution control [8]. Figure 10 shows the spatio-temporal distribution of ozone density. As can be seen in this figure, the ozone density is initially extremely high in the discharge space, which tends to lower values over time because ozone particles effectively participate in the reaction with oxygen atoms (R_{24}) to return to the O_2 state. However, since the density of these particles is of the order of $10^{17}/m^3$ even at low levels and the discharge period is of the order of a few microseconds while the lifetime of these particles is of the order of a few minutes, these particles can remain in the discharge space for some time [9]. Also, according to the figure, it can be seen that the distribution of these particles in the discharge space is almost uniform. Another active particle that plays an important role in the sterilization process is NO radicals.

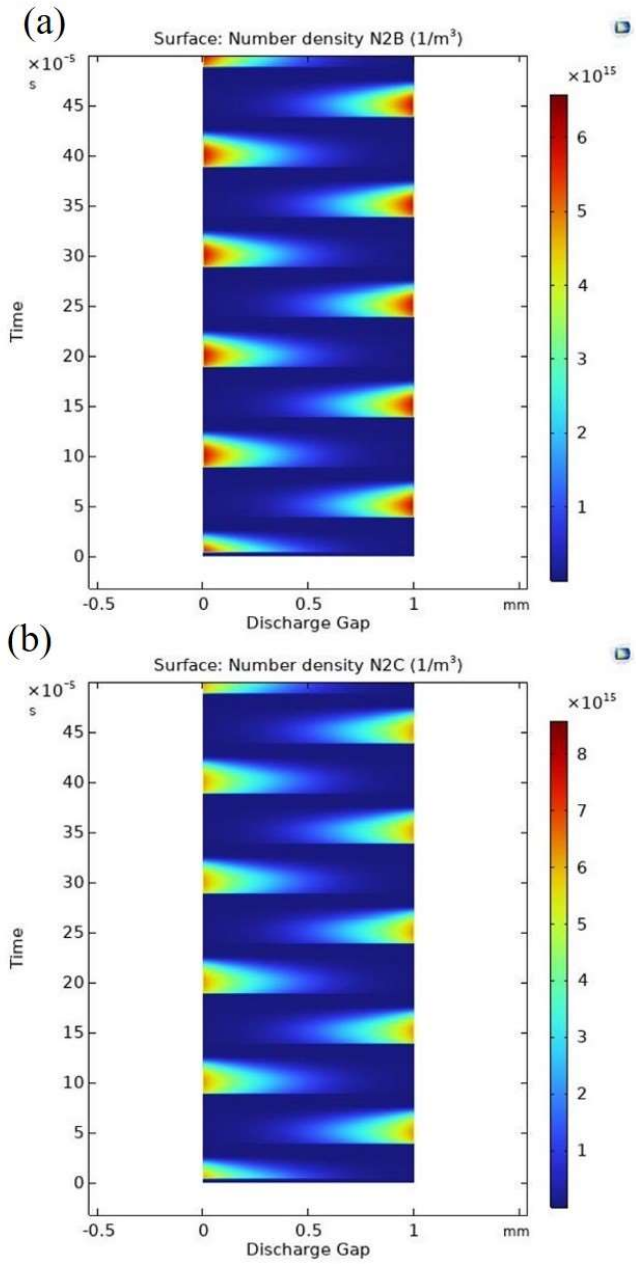


Figure 8 - Spatio-temporal distribution of nitrogen radiation particle density

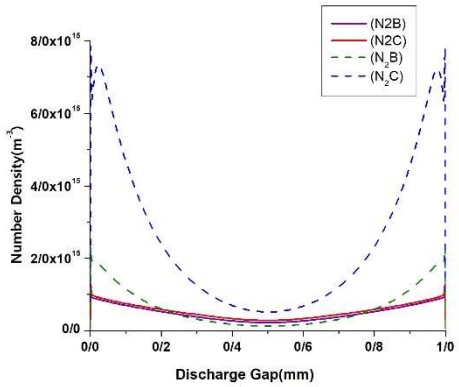


Figure 9. Root mean square of excited particles for discharge with pure nitrogen gas (dashed line) and discharge with a gas mixture of 90% nitrogen - 10% oxygen (solid line)

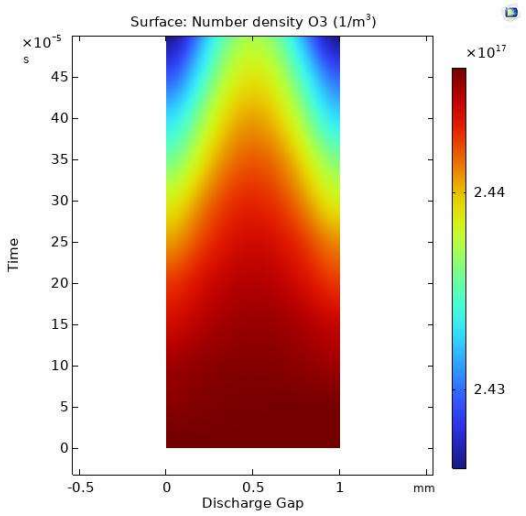


Figure 10. Spatio-temporal distribution of ozone

These particles can easily pass through biological membranes due to their small size and lipophilicity [10]. Thus, these particles also play an important role in the sterilization process. Also, although these particles may be seen as a contaminant in some applications, they play an intermediary role in surface modification because they can be easily adsorbed on the surface and facilitate the nitrogen injection process into the surface [12]. Figure 11 shows the spatio-temporal distribution of the density of NO particles in the evacuation space. As can be seen in this figure, the density of NO particles increases with increasing time in the evacuation space.

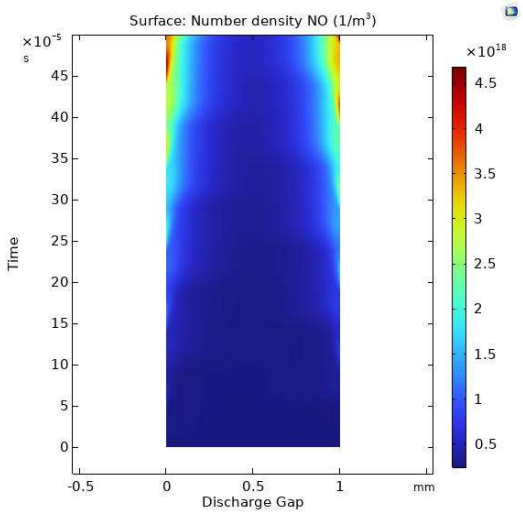


Figure 11- Spatio-temporal distribution of NO in the discharge space

Thus, the presence of these particles improves the quality of surface modification. Another particle that plays an important role in medical applications is oxygen atoms, whose spatio-temporal distribution in this discharge is shown in Figure 12. As can be seen in this figure, the number density of these particles increases with increasing time.

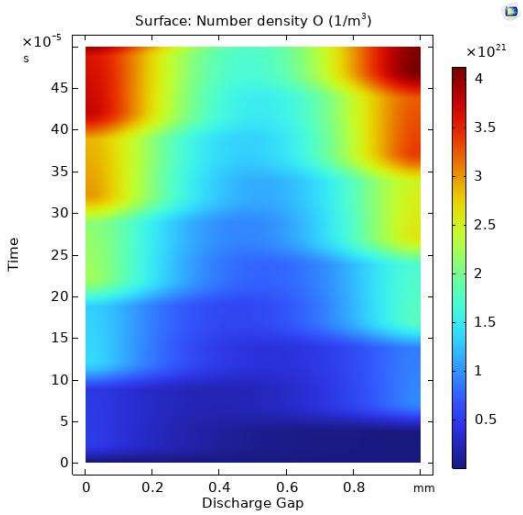


Figure 12 - Spatio-temporal distribution of oxygen atoms

Also, the number of these particles is higher compared to other active particles such as ozone and NO. Therefore, the most important free radical in the 90% nitrogen-10% oxygen discharge is the oxygen radical. These results indicate that this gaseous mixture can be a suitable mixture for

sterilization processes. These particles also play a key role in modifying the surfaces of polymers because these particles, by penetrating the surface of polymers, break the C-H or C-C bonds and replace them with functional groups such as C=O or create hydroxyl groups. Figure 13 shows the comparison of the electron temperature in the discharge with (a) pure nitrogen gas and (b) the gaseous mixture of 90% nitrogen-10% oxygen. As can be seen in this figure, the temperature of the electrons in the discharge with the 90% nitrogen-10% oxygen mixture is higher than the temperature of the electrons in the discharge with pure nitrogen gas. This causes electron reactions to occur more efficiently in a discharge with a gas mixture of 90% nitrogen-10% oxygen than in a discharge in pure nitrogen gas. It can also be seen that in a discharge with pure nitrogen gas, the electron temperature is almost constant throughout all cycles.

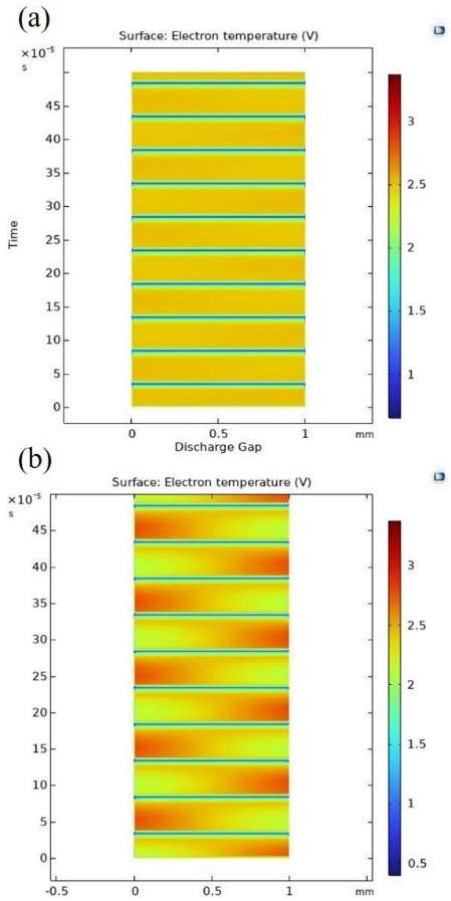


Figure 13. Comparison of electron temperatures in (a) discharge with pure nitrogen gas and (b) discharge with a gas mixture of 90% nitrogen - 10% oxygen**.**

4. DISCUSSION

In this paper, a one-dimensional simulation of dielectric barrier discharge in atmospheric pressure nitrogen gas with the addition of 10% oxygen was performed. It is concluded that the addition of only 10% oxygen increases the number of electrons and their temperature, increases O_2^+ ions, decreases the metastable N_2A particles, increases the metastable N_2a particles, decreases the plasma radiation, produces ozone, increases the density of NO and oxygen free radicals, which makes it a suitable combination for surface modification and sterilization. The increase in electron temperature indicates that the plasma is more chemically active. Thus, the combination of 90% nitrogen-10% oxygen, while producing a relatively stable plasma that does not turn into an arc, spark, or filament discharge despite the presence of 10% oxygen, is also a suitable combination for surface modification and sterilization.

5. REFERENCES

[1] A. Barjasteh, et al., Cold atmospheric pressure plasma: a growing paradigm in diabetic wound healing-mechanism and clinical significance. International Journal of Molecular Sciences, 24 (2023) 16657. DOI: 10.3390/ijms242316657.

[2] A. Barjasteh, et al., Recent progress of non-thermal atmospheric pressure plasma for seed germination and plant development: current scenario and future landscape. Journal of Plant Growth Regulation. 42(2023) 5417–5432. DOI: 10.1007/s00344-023-10979-0.

[3] A. Barjasteh, et al., Cold Atmospheric Pressure Plasma Solutions for Sustainable Food Packaging. International Journal of Molecular Sciences, 25(2024) 6638. DOI: 10.3390/ijms25126638.

[4] Y. Choi, J. Kim, and Y. Hwang, One-dimensional discharge simulation of nitrogen DBD atmospheric pressure plasma. Thin Solid Films. 506 (2006). 389–395.DOI: 10.1016/J.TSF.2005.08.103

[5] T. Kisch., et al., The repetitive use of non-thermal dielectric barrier discharge plasma boosts cutaneous microcirculatory effects. Microvascular Research, 106(2016) 8–13. DOI: 10.1016/j.mvr.2016.02.008.

[6] G. Isbary, et al., A first prospective randomized controlled trial to decrease bacterial load using cold atmospheric argon plasma on chronic wounds in patients. British Journal of Dermatology, 163(2010) 78–82. DOI: 10.1111/j.1365-2133.2010.09744.x.

[7] F. Sohbatzadeh, and H. Soltani, Time-dependent one-dimensional simulation of atmospheric dielectric barrier discharge in $N_2/O_2/H_2O$ using COMSOL Multiphysics. Journal of Theoretical and Applied Physics. 12 (2018) 53–63. DOI: 10.1007/s40094-018-0281-4.

[8] J. Liu, et al., Plasma-assisted ammonia synthesis in a packed-bed dielectric barrier discharge reactor: effect of argon addition .Vacuum, 197 (2022) 110786. DOI: 10.1016/j.vacuum.2021.110786.

[9] M. Akter, et al., Inactivation of infectious bacteria using nonthermal biocompatible plasma cabinet sterilizer. International Journal of Molecular Sciences, 21 (2020) 8321. DOI: 10.3390/ijms21218321.
[10] J. McClurkin, .et al., Half-life time of ozone as a function of air movement and conditions in a sealed container. Journal of Stored Products Research, 55 (2013) 41–47. https://doi.org/10.5073/jka.2010.425.167.326.
[11] C.V. Suschek, et al., The application of cold atmospheric plasma in medicine: The potential role of nitric oxide in plasma-induced effects. Clinical Plasma Medicine, 4 (2016) 1–8. https://doi.org/10.1016/j.cpme.2016.05.001.
[12] O. Nedela, et al., Surface modification of polymer substrates for biomedical applications. *Materials*, 10 (2017) 1115.